

Dynamics near Resonance Junctions in Hamiltonian Systems

Shin-itiro Goto and Kazuhiro Nozaki

Department of Physics, Nagoya University, Nagoya 464-8602, Japan

September 25, 2018

Abstract

An approximate Poincare map near equally strong multiple resonances is reduced by means the method of averaging. Near the resonance junction of three degrees of freedom, we find that some homoclinic orbits “whiskers” in single resonance lines survive and form nearly periodic orbits, each of which looks like a pair of homoclinic orbits.

1 Introduction

In nearly-integrable Hamiltonian systems of three or more degrees of freedom, the KAM tori do not partition phase space into isolated parts and flows diffuse slowly among different resonant tori along the Arnold web (resonance web). This process is known as Arnold diffusion [1], of which time scale is estimated as beyond all order with respect to a small perturbation parameter [2]. The fundamental mechanism for such a diffusion is believed to be provided by a chain of lower-dimensional tori with the transverse intersection of stable and unstable manifolds (“whiskered tori”)[1][3]. Recently, it has been noticed that the believed picture of the Arnold diffusion is justified only away from multiple resonances or resonant junctions and the speed of diffusion is much larger near resonant junctions than that along a single resonance [4]. Near the intersection of a stronger and a weaker resonance, Haller takes advantage of a near-integrable dynamics and constructs a faster motion than that of Arnold diffusion along a single resonance [5].

In this paper, motivated by the above investigations, we reduce an approximate Poincare map near equally strong multiple resonances by means of the method of averaging and study the geometry and dynamics near the resonant junctions. The following significant property is found for a Hamiltonian flow of three degrees of freedom. The two-dimensional stable and unstable manifolds of a hyperbolic fixed point of the Poincare map intersect transversally at homoclinic orbits, which are interpreted as “survivors” of “whiskers” of two-tori on single resonance lines in the Arnold web. Near the homoclinic orbits, there are nearly periodic orbits, each of which looks like a pair of homoclinic orbits. Some implications of such a pair of homoclinic orbits are presented in connection with the Arnold diffusion.

2 Poincare Map near Resonance Junctions

Let us consider the following nearly integrable Hamiltonian in the $2N$ dimensional phase space $(\mathbf{J}, \boldsymbol{\theta})$, where \mathbf{J} and $\boldsymbol{\theta}$ are N dimensional action and phase vectors respectively.

$$H(\mathbf{J}, \boldsymbol{\theta}) = H^0(\mathbf{J}) + \epsilon H^1(\mathbf{J}, \boldsymbol{\theta}),$$

where ϵ is a small parameter and the perturbed Hamiltonian H^1 is assumed to be analytic in the appropriate domain and given by

$$H^1(\mathbf{J}, \boldsymbol{\theta}) = \sum_{\mathbf{m} \in \mathbf{Z}^N} h_{\mathbf{m}}(\mathbf{J}) \exp(i\mathbf{m} \cdot \boldsymbol{\theta}).$$

The frequencies of the unperturbed Hamiltonian H^0 are assumed to satisfy precisely the following “maximal” resonance relationships at some point \mathbf{J}^0 of the action space.

$$\begin{aligned} \mathbf{m}^j \cdot \boldsymbol{\omega}^0 &= 0 \quad (1 \leq j \leq N-1), \\ \mathbf{m}^N \cdot \boldsymbol{\omega}^0 &\neq 0, \end{aligned}$$

where $\boldsymbol{\omega}^0 := \partial H^0 / \partial \mathbf{J}^0$ and \mathbf{m}^j ($j = 1, \dots, N$) are linearly independent integer vectors such that the $N \times N$ matrix

$$M := (\mathbf{m}^1, \mathbf{m}^2, \dots, \mathbf{m}^N),$$

is a unimodular matrix ($\det M = 1$). We introduce the canonical transformation

$$\begin{aligned} \boldsymbol{\theta}' &= M^t \boldsymbol{\theta}, \\ \mathbf{J} &= M \mathbf{J}', \end{aligned}$$

where M^t denotes a transposed matrix of M . Near the resonance point \mathbf{J}^0 or \mathbf{J}'^0 of the action space, the resonance actions (slow variables) J'_j ($1 \leq j \leq N-1$) and the non-resonance action J'_N are scaled as [6]

$$\begin{aligned} J'_j &= J_j^0 + \sqrt{\epsilon} \tilde{J}' + \mathcal{O}(\epsilon) \quad (1 \leq j \leq N-1), \\ J'_N &= J_N^0 + \mathcal{O}(\epsilon). \end{aligned}$$

In the leading order approximation, the Hamiltonian flow near the resonance point \mathbf{J}'^0 is described by

$$\frac{d\theta'_j}{dt} = \sqrt{\epsilon} \sum_{k=1}^{N-1} \tilde{J}'_k f_{kj}^0 + \mathcal{O}(\epsilon) \quad (1 \leq j \leq N-1), \quad (1)$$

$$\frac{d\theta'_N}{dt} = \Omega^0 + \mathcal{O}(\sqrt{\epsilon}), \quad (2)$$

$$\frac{d\tilde{J}'_j}{dt} = -\sqrt{\epsilon} \sum_{\mathbf{m}} im'_j h_{\mathbf{m}}(\mathbf{J}^0) \exp(i\mathbf{m} \cdot \boldsymbol{\theta}') + \mathcal{O}(\epsilon) \quad (1 \leq j \leq N-1), \quad (3)$$

$$\frac{d\tilde{J}'_N}{dt} = \mathcal{O}(\epsilon), \quad (4)$$

where

$$\begin{aligned} f_{kj}^0 &:= \frac{\partial^2 H^0}{\partial J_k^0 \partial J_j^0}, \\ \Omega^0 &:= \mathbf{m}^N \cdot \boldsymbol{\omega}^0. \\ \mathbf{m}' &:= M^{-1} \mathbf{m}. \end{aligned}$$

Since $\Omega^0 \neq 0$ in eq.(2), the non-resonance angle θ'_N is a fast variable, while the resonance variables (J'_j, θ'_j) ($1 \leq j \leq N-1$) are slow variables as seen in eqs.(1) and (3). Integrating eqs.(1) and (3) over a period $T := 2\pi/\Omega^0$ with respect to the fast time so that the symplectic structure is preserved, we have the following Poincare map in the leading order approximation:

$$\begin{aligned} \Delta_+ \tilde{J}'_j(n) &= -i\sqrt{\epsilon}T \sum_{\mathbf{m}} m'_j(\mathbf{m}) h_{\mathbf{m}}(J^0) \\ &\quad \exp(i \sum_{l=1}^{N-1} m'_l(\mathbf{m}) \theta'_l(n)) \delta_{m'_N, 0} \quad (1 \leq j \leq N-1), \end{aligned} \quad (5)$$

$$\Delta_+ \theta'_j(n) = \sqrt{\epsilon}T \sum_{l=1}^{N-1} \tilde{J}'_l(n+1) f_{lj}^{(0)} \quad (1 \leq j \leq N-1), \quad (6)$$

where $\Delta_+ \theta(n) := \theta(n+1) - \theta(n)$ and $n \in \mathbf{N}$. It should be noted that the continuous limit of the approximate Poincare map (5) and (6) becomes the conventional reduced Hamiltonian flow obtained by the method of averaging Hamiltonian in the leading order approximation. Although difference between an asymptotic expression for the Poincare map and an asymptotic averaged Hamiltonian flow is exponentially small in ϵ [7], the exponentially small splitting of a homoclinic orbit can not be described by the asymptotic averaged Hamiltonian flow. Therefore, we take the Poincare map (5) and (6) as the basic system describing the dynamics near the maximal resonance junctions in this paper.

3 Symmetric Hamiltonian with $N = 3$

3.1 Poincare map

As a simple but non-trivial Hamiltonian, we consider $N = 3$ and each degree of freedom represents the same physical motion, that is, the Hamilto-

nian is symmetric with respect to the exchange of a set of canonical variables:

$$\begin{aligned} H(\mathbf{J}, \boldsymbol{\theta}) &= H^0(\mathbf{J}) + \epsilon H^1(\mathbf{J}, \boldsymbol{\theta}), \\ H^0 &= (J_1^2 + J_2^2 + J_3^2)/4, \\ H^1 &= \sum_{\mathbf{m} \in \mathbf{Z}^3} h_{\mathbf{m}} \exp(i\mathbf{m} \cdot \boldsymbol{\theta}), \end{aligned}$$

where

$$h_{(m_1, m_2, m_3)} = h_{(m_2, m_3, m_1)} = h_{(m_3, m_1, m_2)}. \quad (7)$$

Since H^1 is assumed to be analytic so that $h_{\mathbf{m}}$ decays exponentially as $|\mathbf{m}|$ becomes large, we retain Fourier components only for $|m_1| + |m_2| + |m_3| =: |\mathbf{m}| \leq 4$. The maximal resonance junction occurs, for example, at $\mathbf{J}^0 = J^0(1, 1, 1)^t$, i.e. $\boldsymbol{\omega}^0 = \omega^0(1, 1, 1)^t$. Then, linearly independent integer vectors are chosen as

$$\mathbf{m}^1 = (1, -1, 0)^t, \mathbf{m}^2 = (0, 1, -1)^t, \mathbf{m}^3 = (0, 0, 1)^t,$$

where \mathbf{m}^1 and \mathbf{m}^2 generate resonant integer vectors, which are, for example, $\mathbf{m}^1, \mathbf{m}^2, (1, 0, -1)^t, (2, -1, -1)^t, (-1, 2, -1)^t, (-1, -1, 2)^t$ for $|\mathbf{m}| \leq 4$. The Poincare map (5) and (6) becomes

$$\frac{\Delta_+}{\sigma} \tilde{J}'_1(n) = A_J F_J(\theta'_1(n), \theta'_2(n)), \quad (8)$$

$$\frac{\Delta_+}{\sigma} \tilde{J}'_2(n) = A_J F_J(\theta'_2(n), \theta'_1(n)), \quad (9)$$

$$\frac{\Delta_+}{\sigma} \theta'_1(n) = A_\theta F_\theta(\tilde{J}'_1(n+1), \tilde{J}'_2(n+1)), \quad (10)$$

$$\frac{\Delta_+}{\sigma} \theta'_2(n) = A_\theta F_\theta(\tilde{J}'_2(n+1), \tilde{J}'_1(n+1)), \quad (11)$$

where

$$\begin{aligned} F_J(\theta'_1, \theta'_2) &:= \sin(\theta'_1) + \sin(\theta'_1 + \theta'_2) + 2\tilde{h}_2\{\sin(2\theta'_1) + \sin(2\theta_1 + 2\theta'_2)\} + \\ &\quad \tilde{h}_3\{2\sin(2\theta' + \theta'_2) + \sin(\theta'_1 - \theta'_2) + \sin(\theta'_1 + 2\theta'_2)\}, \\ F_\theta(\tilde{J}'_1, \tilde{J}'_2) &:= \tilde{J}'_1 - \tilde{J}'_2/2 \\ \sigma &:= \sqrt{2\epsilon T^2 h_1}, \\ A_J &:= \sqrt{2h_1}, \quad A_\theta := 1/A_J, \\ h_1 &= h_{(1, -1, 0)} = \cdots, \quad h_2 = h_{(2, -2, 0)} = \cdots, \quad h_3 = h_{(2, -1, -1)} = \cdots, \\ \tilde{h}_2 &:= h_2/h_1, \quad \tilde{h}_3 := h_3/h_1. \end{aligned}$$

3.2 Geometry near Resonance Junction

The map (8)-(11) has a hyperbolic fixed point $(\tilde{J}'_1, \tilde{J}'_2, \theta'_1, \theta'_2) = (0, 0, 0, 0)$, which is the resonance junction. Degenerate eigenvalues of the linearized map at the fixed point are given by

$$\begin{aligned}\lambda^u &:= 3H\sigma^2/4 + 1 + \sqrt{9H^2\sigma^4 + 24H\sigma^2}/4, \\ \lambda^s &:= 3H\sigma^2/4 + 1 - \sqrt{9H^2\sigma^4 + 24H\sigma^2}/4,\end{aligned}$$

where $H := 1 + 4\tilde{h}_2 + 3\tilde{h}_3$. The linearized stable (W^s) and unstable (W^u) manifolds of the fixed point are

$$W^{s,u} = c_1^{s,u} \begin{pmatrix} E^{s,u} \\ 2E^{s,u} \\ 0 \\ 1 \end{pmatrix} + c_2^{s,u} \begin{pmatrix} 2E^{s,u} \\ E^{s,u} \\ 1 \\ 0 \end{pmatrix}, \quad (12)$$

$$E^{s,u} := \frac{2(1 - \lambda^{u,s})}{3A_\theta\sigma}, \quad c_1^{s,u}, c_2^{s,u} \in \mathbf{R}$$

It is easy to show that the map (8)-(11) has the following homoclinic orbits γ_j ($j = 1, \dots, 6$), which connect the hyperbolic fixed point $(0, 0, 0, 0)$ to itself.

orbit	$c1:c2$	\tilde{J}'	θ'	\tilde{J}
γ_1	1: 1	$\tilde{J}'_1 = \tilde{J}'_2$	$\theta'_1 = \theta'_2 = S_2$	$\tilde{J}_1 = -\tilde{J}_3, \tilde{J}_2 = 0$
γ_2	-2: 1	$\tilde{J}'_1 = 0$	$2\theta'_1 + \theta'_2 = 0, \theta'_1 = S_2$	$\tilde{J}_3 = -\tilde{J}_2, \tilde{J}_1 = 0$
γ_3	1:-2	$\tilde{J}'_2 = 0$	$\theta'_1 + 2\theta'_2 = 0, \theta'_2 = S_2$	$\tilde{J}_2 = -\tilde{J}_1, \tilde{J}_3 = 0$
γ_4	1:-1	$\tilde{J}'_2 = -\tilde{J}'_1$	$\theta'_1 + \theta'_2 = 0, \theta'_1 = S_1$	$\tilde{J}_3 = \tilde{J}_1, 2\tilde{J}_1 + \tilde{J}_2 = 0$
γ_5	0: 1	$\tilde{J}'_2 = 2\tilde{J}'_1$	$\theta'_2 = 0, \theta'_1 = S_1$	$\tilde{J}_2 = \tilde{J}_3, 2\tilde{J}_3 + \tilde{J}_2 = 0$
γ_6	1: 0	$\tilde{J}'_2 = \tilde{J}'_1$	$\theta'_1 = 0, \theta'_2 = S_1$	$\tilde{J}_1 = \tilde{J}_2, 2\tilde{J}_2 + \tilde{J}_3 = 0$

Here, $c1 : c2$ indicates the direction of each homoclinic orbit near the fixed point (see eq.(12)), $J_j = J_j^0 + \sqrt{\epsilon}\tilde{J}_j + \mathcal{O}(\epsilon)$ and S_1, S_2 are homoclinic solutions of the following two-dimensional maps similar to the standard map.

$$\begin{aligned}\frac{\Delta^2}{\sigma^2}S_2(n) &= \frac{1}{2}\{\sin S_2(n) + (1 + 2\tilde{h}_2)\sin 2S_2(n) \\ &\quad + 3\tilde{h}_3\sin 3S_2(n) + 2\tilde{h}_2\sin 4S_2(n)\},\end{aligned} \quad (13)$$

$$\frac{\Delta^2}{\sigma^2}S_1(n) = \frac{3}{2}\{(1 + \tilde{h}_3)\sin S_1(n) + (2\tilde{h}_2 + \tilde{h}_3)\sin 2S_1(n)\}, \quad (14)$$

where $\Delta^2 S(n) := S(n+1) + S(n-1) - 2S(n)$.

Six homoclinic orbits γ_j ($j = 1, \dots, 6$) are classified into two types according to two homoclinic solutions S_1, S_2 , i.e. the type of γ_j ($j = 1, 2, 3$) and γ_j ($j = 4, 5, 6$) are considered to be different from each other.

Thus, we obtain a geometrical picture of invariant manifolds near the resonance junction such that the hyperbolic fixed point at the junction has two-dimensional stable and unstable manifolds, of which tangent spaces are given by eq.(12). The two-dimensional stable and unstable manifolds are shown to intersect transversally at the homoclinic orbits γ_j ($j = 1, \dots, 6$) (an infinite number of homoclinic points), which produce stochastic layers with exponentially small widths [8] [9]. If we take the continuous limit of (13) and (14), the exponentially small effects with respect to ϵ are neglected and the above homoclinic orbits are reduced to homoclinic lines without stochastic layers. In the next subsection, the homoclinic orbits γ_j ($j = 1, \dots, 6$) are interpreted as “survivors” of homoclinic orbits (“whiskers”) associated with two-tori in single resonances.

3.3 Whiskered Tori in Single Resonances

Let us consider a single resonance line connected to the present resonance junction: for example, set $\mathbf{J}^0 = J^0(1, 1, r)^t$ and $\boldsymbol{\omega}^0 = \Omega^0(1, 1, r)^t$, where r is an irrational number near 1. Then, the resonant integer vector is $\mathbf{m}^1 = (1, -1, 0)^t$ and $\boldsymbol{\omega}^0 \cdot \mathbf{m}^1 = 0$, while $\boldsymbol{\omega}^0 \cdot \mathbf{m}^2 \neq 0$ and $\boldsymbol{\omega}^0 \cdot \mathbf{m}^3 \neq 0$. Since θ'_1 is a only slowly varying phase, we average eqs.(8)-(11) over a fast varying phase θ'_2 . We have $\tilde{J}'_2 = 0$ and

$$\begin{aligned}\Delta_+ \tilde{J}'_1(n) &= A_J \sigma \{ \sin \theta'_1(n) + 2\tilde{h}_2 \sin 2\theta'_2(n) \}, \\ \Delta_+ \theta'_1(n) &= A_\theta \sigma \tilde{J}'_1(n+1),\end{aligned}$$

which is the standard map and has a homoclinic orbit connecting a hyperbolic fixed point $\theta'_1 = 0 \pmod{2\pi}$, $\tilde{J}'_1 = 0$. The two torus characterized by $\tilde{J}'_2, \tilde{J}'_3$ is called a whiskered torus associated with a homoclinic orbit (“a whisker”) (\tilde{J}'_1, θ'_1). From the canonical transformation

$$\begin{pmatrix} \tilde{J}'_1 \\ \tilde{J}'_2 \\ \tilde{J}'_3 \end{pmatrix} = \begin{pmatrix} \tilde{J}_1 \\ \tilde{J}_1 + \tilde{J}_2 \\ \tilde{J}_1 + \tilde{J}_2 + \tilde{J}_3 \end{pmatrix}$$

and $\tilde{J}'_2 = \tilde{J}'_3 = 0$, we have

$$\tilde{J}_1 = -\tilde{J}_2, \quad \tilde{J}_3 = 0,$$

which is the relation of the homoclinic orbit γ_3 in the resonant junction. In this sense, the homoclinic orbit γ_3 is interpreted as a survivor of the homoclinic orbit (“whisker”) on the single resonance line specified by the resonant integer vector $\mathbf{m}^1 = (1, -1, 0)^t$.

Similar discussions near the other single resonance lines connected to the resonance junction yield the following correspondence between the homoclinic orbits γ_j ($j = 1, \dots, 6$) and “whiskers” of two-tori in single resonances.

orbit	type	$\boldsymbol{\omega}^0/\Omega^0$	\mathbf{m}
γ_1	S_2	(1,r,1)	(1, 0, -1)
γ_2	S_2	(r, 1, 1)	(0, -1, 1)
γ_3	S_2	(1,1,r)	(-1, 1, 0)
γ_4	S_1	(1 + r', 1, 1 - r')	(-1, 2, -1)
γ_5	S_1	(1, 1 - r', 1 + r')	(2, -1, -1)
γ_6	S_1	(1 - r', 1 + r', 1)	(-1, -1, 2)

All possible “whiskers” on single resonance lines connected to the present resonance junction survive as the homoclinic orbits γ_j , ($j = 1, \dots, 6$). Therefore, the two different types of homoclinic orbit correspond to different single resonances, that is γ_j ($j = 1, 2, 3$) corresponds to (1, -1, 0) etc. and γ_j ($j = 4, 5, 6$) to (2, -1, -1) etc.

3.4 A Pair of Homoclinic Orbits

In order to study dynamics near the homoclinic orbits in the resonant junction, we set initial values for the map (8)-(11) close to each homoclinic orbit γ_j and obtain numerical solutions. As shown in Fig.(1), we find a nearly periodic orbit which looks like a pairing of two types of homoclinic orbits γ_1 and γ_4 . Hereafter, such a periodic orbit is called a pair of homoclinic orbits for short. Similar numerical calculations as Fig.(1) indicates that each homoclinic orbit has the definite one as a pair such that (γ_1, γ_4) , (γ_2, γ_5) and (γ_3, γ_6) . The type of homoclinic orbit in the pair is different from each other. Implications of such a pair of homoclinic orbits are discussed in the last section in connection with the Arnold diffusion near resonant junctions.

4 Asymmetric Hamiltonian with $N = 3$

In stead of the symmetry condition (7), we set

$$\begin{aligned} h &:= h_{(1,-1,0)} = h_{(-1,1,0)} = h_{(0,1,-1)} = h_{(0,-1,1)}, \\ h_C &:= h_{(1,0,-1)} = h_{(-1,0,-1)} \neq h, \end{aligned}$$

and $h_{\mathbf{m}} = 0$ for $|\mathbf{m}| > 2$. Then, the Hamiltonian becomes slightly asymmetric and we have the following Poincare map near the resonance junction $\mathbf{J}^0 = \mathcal{J}^0(1, 1, 1)^t$.

$$\frac{\Delta_+}{\hat{\sigma}} \tilde{J}'_1(n) = 2h \sin(\theta'_1(n)) + 2h_C \sin(\theta'_1(n) + \theta'_2(n)), \quad (15)$$

$$\frac{\Delta_+}{\hat{\sigma}} \tilde{J}'_2(n) = 2h \sin(\theta'_2(n)) + 2h_C \sin(\theta'_1(n) + \theta'_2(n)), \quad (16)$$

$$\frac{\Delta_+}{\hat{\sigma}} \theta'_1(n) = \tilde{J}'_1(n+1) - \tilde{J}'_2(n+1)/2, \quad (17)$$

$$\frac{\Delta_+}{\hat{\sigma}} \theta'_2(n) = \tilde{J}'_2(n+1) - \tilde{J}'_1(n+1)/2, \quad (18)$$

where $\hat{\sigma} := \sqrt{\epsilon T}$. The map (15)-(18) has the same fixed point as that of (8)-(11). Eigenvalues of the linearized map at the fixed point have four distinct values given by

$$\lambda_4^u = 1 + 3\hat{\sigma}^2 h/2 + \sqrt{12\hat{\sigma}^2 h + 9\hat{\sigma}^4 h^2}/2,$$

$$\lambda_4^s = 1 + 3\hat{\sigma}^2 h/2 - \sqrt{12\hat{\sigma}^2 h + 9\hat{\sigma}^4 h^2}/2,$$

$$\lambda_1^u = \hat{\sigma}^2 h/2 + \hat{\sigma}^2 h_C + 1 + \sqrt{\hat{\sigma}^4 h^2 + 4\hat{\sigma}^2 h_C h + 4\hat{\sigma}^2 h + 4\hat{\sigma}^4 h_C^2 + 8\hat{\sigma}^2 h_C}/2,$$

$$\lambda_1^s = \hat{\sigma}^2 h/2 + \hat{\sigma}^2 h_C + 1 - \sqrt{\hat{\sigma}^4 h^2 + 4\hat{\sigma}^2 h_C h + 4\hat{\sigma}^2 h + 4\hat{\sigma}^4 h_C^2 + 8\hat{\sigma}^2 h_C}/2.$$

The tangent spaces of the local stable and unstable manifolds of the fixed point are two-dimensional vector space generated by eigenvectors W_j^s and W_j^u associated with λ_j^s and λ_j^u respectively, where

$$W_4^u = \begin{pmatrix} -E_4^u \\ E_4^u \\ 1 \\ -1 \end{pmatrix}, \quad W_4^s = \begin{pmatrix} -E_4^s \\ E_4^s \\ 1 \\ -1 \end{pmatrix}.$$

$$W_1^u = \begin{pmatrix} E_1^u \\ E_1^u \\ 1 \\ 1 \end{pmatrix}, \quad W_1^s = \begin{pmatrix} E_1^s \\ E_1^s \\ 1 \\ 1 \end{pmatrix}.$$

where

$$E_4^{s,u} := \frac{2}{3\hat{\sigma}}(\lambda_4^{u,s} - 1), \quad E_1^{s,u} := \frac{-2}{\hat{\sigma}}(\lambda_1^{u,s} - 1).$$

In this case, we have the following two homoclinic orbits $\hat{\gamma}_4, \hat{\gamma}_1$.

$$\begin{aligned} \hat{\gamma}_4 &: \tilde{J}'_1 = -\tilde{J}'_2, \theta'_1 = -\theta'_2 = \hat{S}_1, \quad \frac{\Delta^2}{\hat{\sigma}^2} \hat{S}_1(n) = 3h \sin \hat{S}_1(n). \\ \hat{\gamma}_1 &: \tilde{J}'_1 = \tilde{J}'_2, \theta'_1 = \theta'_2 = \hat{S}_2, \quad \frac{\Delta^2}{\hat{\sigma}^2} \hat{S}_2(n) = h \sin \hat{S}_2(n) + h_C \sin 2\hat{S}_2(n), \end{aligned}$$

It should be noted that the directions of $\hat{\gamma}_4, \hat{\gamma}_1$ near the fixed point are identical with eigen-vectors $W_4^{s,u}, W_1^{s,u}$ respectively and $\hat{\gamma}_4, \hat{\gamma}_1$ correspond to γ_4, γ_1 in the symmetrical case.

If we set initial values at arbitrary points close to the fixed point, the homoclinic orbit ($\hat{\gamma}_4$) in the direction of the eigenvector with the largest eigenvalue (λ_4^u) is first observed and the other homoclinic orbit follows as shown in Fig.(2). Thus, a pairing of homoclinic orbits are also observed in this case. However, the correspondence between homoclinic orbits in the resonance junction and whiskers in single resonance lines is restricted.

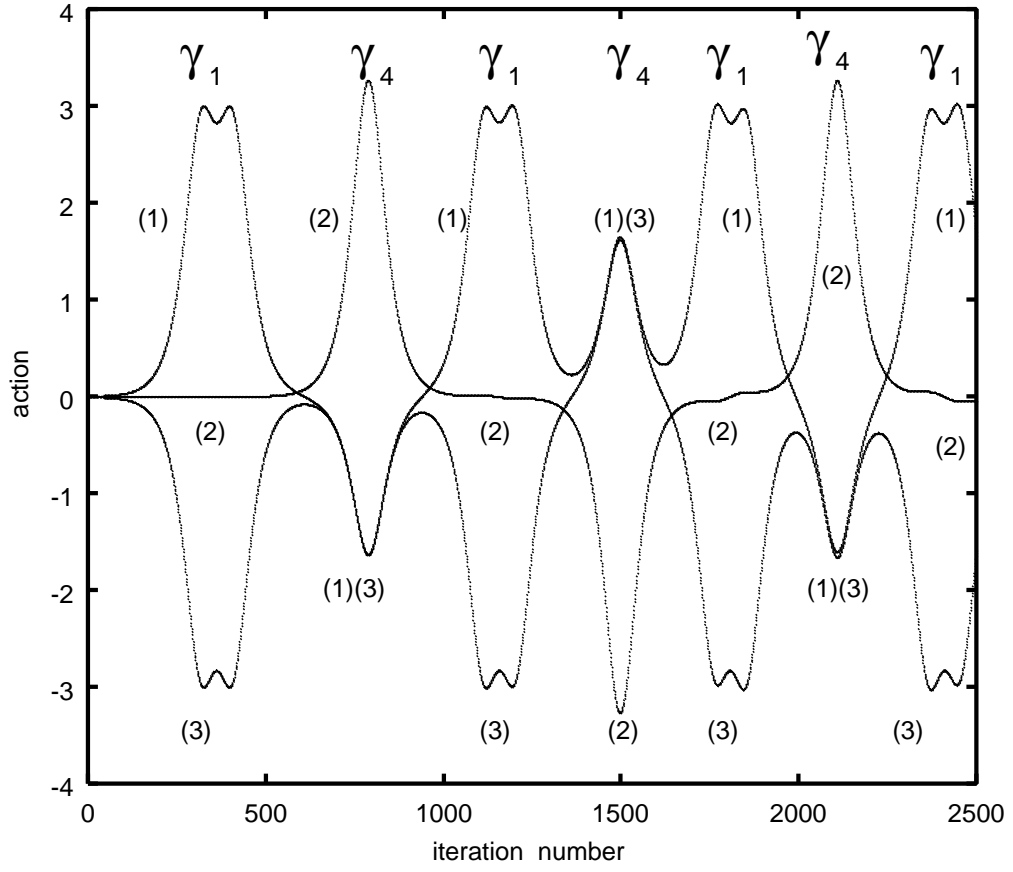


Figure 1: A nearly periodic orbit of a pair $(\hat{\gamma}_1, \hat{\gamma}_4)$ for $\sigma = 0.02, A_J = A_\theta = 1, h_2 = h_3 = 0.001$. where (1)(2) and (3) denote $\tilde{J}_1(n), \tilde{J}_2(n)$ and $\tilde{J}_3(n)$ respectively.

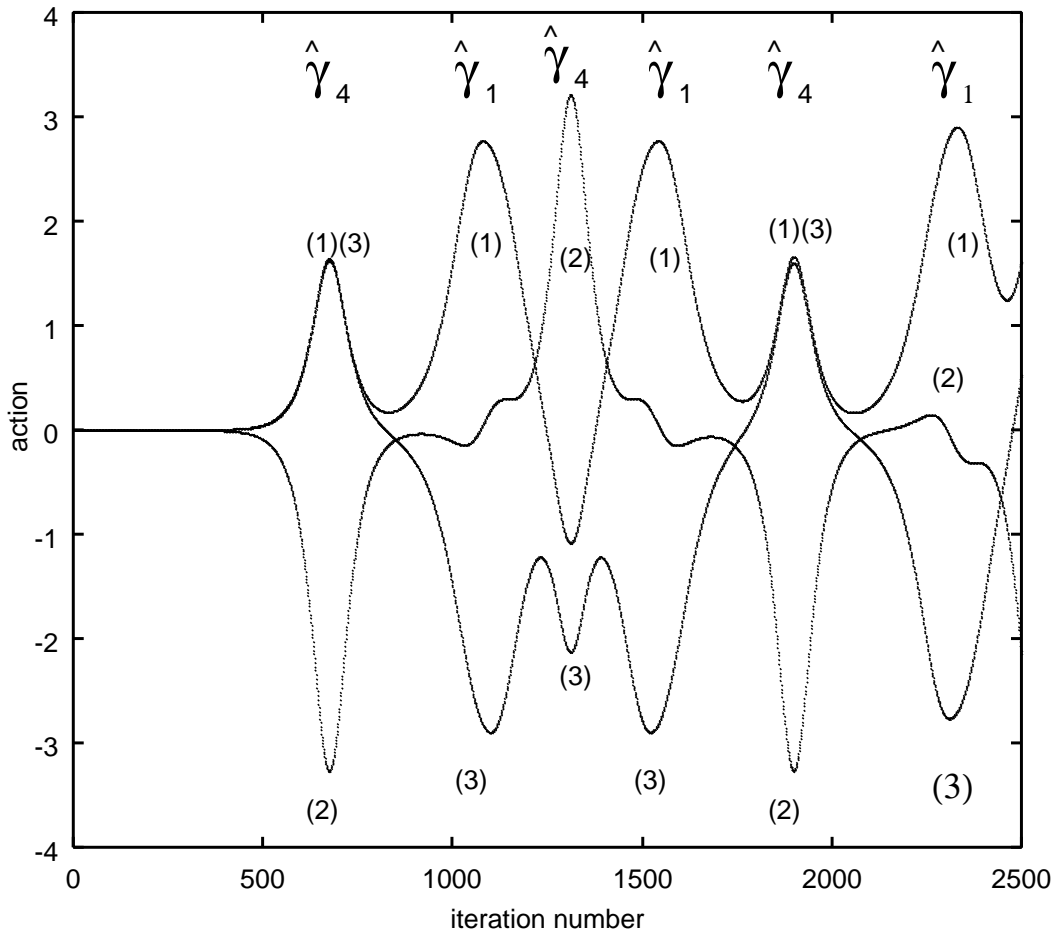


Figure 2: A nearly periodic orbit of a pair $(\hat{\gamma}_1, \hat{\gamma}_4)$ for $\hat{\sigma} = 0.02, h = 0.5, h_C = 0.1$. where (1)(2) and (3) denote $\tilde{J}_1(n), \tilde{J}_2(n)$ and $\tilde{J}_3(n)$ respectively.

5 Discussion

For a symmetrical Hamiltonian system with three degrees of freedom, we find the following significant property. The maximal resonance junction is a hyperbolic fixed point of the Poincare map. The two-dimensional stable and unstable manifolds of the fixed point intersect transversally at six homoclinic orbits, which are interpreted as “survivors” of “whiskers” of two-tori on single resonance lines in the Arnold web. Near the homoclinic orbits, there are three nearly periodic orbits, each of which looks like a pair of homoclinic orbits. Let us consider implications of such a pair of homoclinic orbits in connection with the Arnold diffusion near resonant junctions. The conventional Arnold diffusion occurs along a single resonance line, say, $\mathbf{J}^0 = J^0(1, r, 1)^t$. The value of irrational r varies very slowly due to a whisker of γ_1 type. If r reaches 1, \mathbf{J}^0 plunges into the resonance junction and the whisker of γ_1 type turns into the homoclinic orbit γ_1 . Then, a pairing of homoclinic orbits occurs and a periodic orbit of homoclinic orbits (γ_1, γ_4) forms in the way shown in Fig.(1). After a long excursion along the nearly periodic orbit, the system will leave the resonant junction and diffuses again along a single resonance line with a whisker γ_1 or γ_4 . Thus, a pairing of homoclinic orbits at the resonant junction may give a selection rule for the transition among different single resonances.

Although the above implications of a pair of homoclinic orbits are for the symmetrical Hamiltonian system, similar implications are provided for a pair of homoclinic orbits $(\hat{\gamma}_1, \hat{\gamma}_4)$ in the asymmetrical Hamiltonian system. Furthermore, such a pair of homoclinic orbits will play an important role in an understanding of dynamics in the Arnold web in general.

References

- [1] V.I.Arnold, Sov.Math.Dokl.5,581 (1964)
- [2] N.N.Nekhoroshev, Usp.Mat.Nauk.USSR 32,6 (1977)
- [3] P.J.Holmes and J.E.Marsden, J.Math.Phys.23,669(1982).
- [4] J.Laskar, Physica D 67,257(1993).
- [5] G.Haller, Phys.Lett.A200,34(1994).

- [6] for example, A.J.Lichtenberg and M.A.Lieberman, “Regular and Stochastic Motion” Springer-Verlag:New York,Heidelberg,Berlin.
- [7] A.I.Neishtadt,J.Appl.Math.Mech.48,133(1984).
- [8] V.G.Gelfreich,D.K.Sharomov,Phys.Lett.A197,139(1995).
- [9] Y.Hirata,K.Nozaki and T.Konishi, Prog.Theor.Phys.101,1181 (1999).